

## Distribution of Shape-Changing Compounds across the Red Cell Membrane<sup>†</sup>

Edmund D. Matayoshi\*

**ABSTRACT:** The effects of two oppositely charged pyrene derivatives, 1-pyrenebutylcholine (PBC) and 1-pyrenebutyric acid (PBA), on red blood cell shape have been examined. Both compounds convert normal biconcave erythrocytes into echinocytes. However, with extended incubation time at elevated temperature, the morphology of PBC-induced echinocytes is reversed. Examination of probe uptake confirmed that, in contrast to PBA, equilibration of PBC with intact cells occurs very slowly. For PBA-induced echinocytes, it was possible to quantitate the fraction of probe bound in each half of the bilayer from nanosecond fluorescence measurements. Analysis of the heterogeneous decay showed that 71% of the bound PBA was associated with a lifetime ( $\tau$ ) of 102 ns and 29% with  $\tau = 8$  ns. It is likely that the latter, highly quenched, component corresponds to fluorophores bound at the cytoplasmic surface because of efficient energy transfer to hemoglobin and that the long component corresponds to probe

bound exclusively at the outer surface. Evidence in support of this interpretation was obtained by showing that when the paramagnetic cation  $Mn^{2+}$  is bound at the extracellular surface the 102-ns component is quenched. The excimer fluorescence of PBC bound to red cells was examined and found to show time and temperature dependencies which correlate with morphological effects. These results indicate that red cells become crenated when PBC molecules are highly concentrated in the outer bilayer half and that shape reversal is subsequently brought about as PBC permeates and accumulates in the inner bilayer half. Finally, hemolysis protection due to PBC or PBA binding was observed also to show striking correlations with cell shape. In summary, these findings support the hypothesis [Sheetz, M. P., & Singer, S. J. (1974) *Proc. Natl. Acad. Sci. U.S.A.* 71, 4457] that shape changes are induced in red cells by amphiphilic molecules as a consequence of their relative partitioning between the two halves of the bilayer.

It has long been appreciated that the ability of human erythrocytes to maintain their biconcave disk shape is governed by structural properties of the membrane. A variety of phenomena will induce normal discocytes to undergo transformation to crenated ("echinocytic") or cupped ("stomatocytic") shapes, for example, ATP depletion, accumulation of intracellular calcium, changes in pH, and exposure to glass surfaces (Brecher & Bessis, 1972; Bessis et al., 1973). In addition, red cell shape is altered by a diverse number of chemically unrelated amphiphilic drugs and organic compounds. The correlation between the charge of these substances and their effect on shape was first pointed out by Deuticke (1968)—the crenators are usually anionic or nonionized amphiphiles whereas the cup formers are almost exclusively cationic amphiphiles. Crenated or cupped cells, induced by any means, are readily reversed by the addition of cupping or crenating agents, respectively.

Sheetz & Singer (1974) extended these observations by hypothesizing that crenation and cupping were the result of an asymmetric expansion or contraction of the surface areas of the two bilayer halves relative to one another, leading to the observed inward or outward curvature of the membrane. The asymmetrically distributed phospholipids of the human erythrocyte membrane (Zwaal et al., 1975) could provide the structural basis for the action of shape-changing compounds. The cationic cupping compounds might preferentially partition into the cytoplasmic half of the bilayer because of the negative field which arises from phosphatidylserine. The crenating compounds, however, would concentrate in the outer half (which contains mainly phosphatidylcholine and sphingomyelin, but no phosphatidylserine) due either to repulsion from the inner half or to an inability to permeate the bilayer. The

Sheetz and Singer "bilayer-couple hypothesis" was based on their experiments comparing the shape-inducing effects of the tertiary phenothiazine chlorpromazine and its quaternary analogue methochlorpromazine (Sheetz & Singer, 1974, 1976; Sheetz et al., 1976). Both drugs induce cupping of unsealed ghosts and chlorpromazine cups intact cells as well, but methochlorpromazine initially converts intact cells into echinocytes. Under certain conditions, the latter shape change can be reversed and intact cells transformed to stomatocytes. Drug binding was not quantitated, but these results could be explained by assuming that the positively charged methochlorpromazine is only poorly permeable to intact cells and therefore reaches equilibrium with the inner bilayer half very slowly; in contrast, chlorpromazine could permeate rapidly via its discharged (unprotonated) form.

In the work presented here, we have attempted to test the bilayer-couple hypothesis by examining the effects of two amphiphilic pyrene derivatives, 1-pyrenebutylcholine (PBC)<sup>1</sup> and 1-pyrenebutyric acid (PBA), on the shape of human erythrocytes. Because these two compounds differ only in the nature of their charged moieties, they were anticipated to induce a number of contrasting effects on cell morphology. The nonpolar pyrene group provides these compounds with several useful fluorescent properties which enabled us to study their membrane distribution and its relationship to cell shape.

### Materials and Methods

1-Pyrenebutyric acid (PBA) was obtained from Eastman Organic Chemicals (Rochester, NY) and was recrystallized from ethanol-water before use; 1-pyrenebutylcholine (PBC) bromide was a product of Molecular Probes (Plano, TX) and was used as supplied. The probes contained no fluorescent impurities as judged by thin-layer chromatography, their homogeneous fluorescent lifetimes in ethanol, and the observation that their fluorescence spectra were independent of excitation wavelength. Neither PBA nor PBC displays

<sup>†</sup> From the Biophysical Laboratory, Harvard Medical School, Boston, Massachusetts 02115. Received February 5, 1980. This research was supported by Grants HL14820 and 5 T01 GM00782-20 to A. K. Solomon from the National Institutes of Health.

\* Present address: Max Planck Institut für Biophysikalische Chemie, Abteilung Molekulare Biologie, Göttingen, Federal Republic of Germany. Reprint requests should be sent to Harvard Medical School.

<sup>1</sup> Abbreviations used: PBA, 1-pyrenebutyric acid; PBC, 1-pyrenebutylcholine.

emission wavelength dependent lifetimes under any of the conditions of the experiments described in this paper. However, as will be discussed below, an emission monochromator was always used in order to minimize scattering contributions to the fluorescence signal.

Both probes were dissolved in *N,N*-dimethylformamide as 0.1 M stock solutions. Aqueous dispersions of each were prepared, just before the labeling of cells, by adding microliter quantities of stock solutions to the desired buffer (1000-fold or great dilution) under vigorous vortexing. For all PBC experiments, it was necessary to use plastic test tubes and pipets (Falcon 2057 and 7543, Fisher Scientific, Pittsburgh, PA) because of apparent absorption of PBC to glassware.

Fresh human blood was obtained by venipuncture into heparin and used within a day. The plasma was removed, and the erythrocytes were washed in phosphate-buffered saline (10 mM sodium phosphate and 150 mM sodium chloride, pH 7.4). Unsealed, hemoglobin-free ghosts were prepared by hemolysis of washed cells at 4 °C with 20 volumes of 10 mM sodium phosphate, pH 7.4, followed by several washes in the same buffer or in 10 mM Tris-HCl and 10 mM NaCl, pH 7.4. Ghosts were assayed for protein content by the method of Lowry et al. (1951) and for phospholipid concentration (determined as inorganic phosphate) by the method of Gomori (1942).

Cell shape was assessed by light microscopy after fixation for at least 1 h at 0 °C in 1% glutaraldehyde and phosphate-buffered saline, pH 7.4, at an approximately 2% hematocrit. The cell-shape nomenclature employed here is that defined and illustrated by Bessis (1973). Increasing distortion of cell shape by crenating agents follows the transformation sequence discocyte → echinocytes I, II, III → spherocytocytes I, II → spherocyte, and the transformation of cells by cupping agents follows the sequence described as discocyte → stomatocytes I, II → spherostomatocytes I, II → spherocyte.

**Uptake Measurements.** Washed red cells or ghosts were added to aqueous dispersions of PBA and PBC, and probe partitioning was measured by centrifugation and sampling of the supernatant. The supernatant was measured for PBA or PBC by absorption at 342 nm, with a molar extinction coefficient of  $4 \times 10^4 \text{ M}^{-1} \text{ cm}^{-1}$ . When necessary, a correction for hemoglobin absorbance at 342 nm was made, as inferred from the hemoglobin absorbance at 540 nm (where pyrene has no absorbance). Uptake into intact cells as a function of time was measured by sampling suspensions of cells incubating in a water bath at various time points, centrifuging within seconds in a Brinkmann microcentrifuge (Eppendorf Model 3200), and measuring the supernatant for pyrene content.

**Partition Coefficients.** The membrane partition coefficient ( $K_p$ ) is defined as  $K_p = C_m/C_w$ , where  $C_m$  is the concentration (mol/L) of probe in the membrane and  $C_w$  is the concentration of probe in the aqueous phase. Since the concentration of probe in the total solution ( $C$ ) is  $C = (C_m V_m + C_w V_w)/(V_m + V_w)$ , where  $V_m$  is the volume of the membrane phase and  $V_w$  the volume of the aqueous phase, it follows that  $K_p$  is given by

$$K_p = \frac{V_w}{V_m} \left[ \frac{C}{C_w} \left( 1 + \frac{V_m}{V_w} \right) - 1 \right]$$

The volume assumed for a single red cell membrane was  $10.1 \times 10^{-13} \text{ cm}^3$ , which corresponds to  $1.68 \text{ cm}^3/\text{g}$  of membrane protein. This value was obtained by assuming the following protein, lipid, and carbohydrate content for the red cell membrane:  $6 \times 10^{-13} \text{ g}$  of protein/cell (Dodge et al., 1964),  $5.0 \times 10^{-13} \text{ g}$  of lipid/cell (Van Deenen & DeGier, 1974), and

$1.0 \times 10^{-13} \text{ g}$  of carbohydrate/cell (Guidotti, 1972). The densities ( $\text{g}/\text{cm}^3$ ) assumed were 1.35 (protein), 1.00 (lipid), and 1.54 (carbohydrate). An overall membrane density of 1.17 (Kwant & Seeman, 1969), taken with the above value of 6 g of membrane protein/12 g of membrane, implies a similar membrane volume. For intact erythrocytes, the cell number was determined from the hematocrit and an assumed value of  $8.6 \times 10^{-11} \text{ cm}^3/\text{cell}$  (Diem & Lentner, 1970). The cell number in dilute suspensions of cells (<20% hematocrit) was determined by hemoglobin content (relative to concentrated suspensions) after conversion to cyanomethemoglobin by a standard Drabkin's solution.

**Hemolysis Protection.** Washed cells were incubated with PBA or PBC (time and temperature indicated in figures) at a hematocrit of 1–2% and then diluted into a hypotonic solution containing the same concentration of drug. Care was taken to do the hemolyses at constant temperature because the hemolytic fragility of human erythrocytes is a function of temperature (Aloni et al., 1977). The NaCl concentration of the diluting solution was adjusted to produce about 30% hemolysis of control (untreated) cells after 10 min at room temperature. The extent of hemolysis was measured by pelleting samples in the microcentrifuge and measuring the absorbance of the supernatant at 540 nm. Results are reported as relative hemolysis, i.e., fractional hemolysis relative to control cells.

**Fluorescence Measurements.** Fluorescence lifetimes were determined by the phase-modulation technique in an instrument built by SLM Instruments (Urbana, IL). Both lifetime and steady-state measurements on intact erythrocytes could be performed in this apparatus by use of a front-surface optical geometry. A sample holder was constructed which positioned the front face of one cuvette at a 60° angle from the illuminating beam, and emission was detected from the same face. The second position of the sample holder accommodated a cuvette in the normal 90° geometry. This second position was used to hold the glycogen-scattering solution in lifetime measurements or a reference-intensity solution for steady-state measurements. Constant temperature was maintained by connection to an external-circulating water bath.

The theory of phase and modulation fluorometry has been discussed in detail before (Birks, 1970; Spencer, 1970). For a homogeneous system with single exponential decay, the lifetimes determined by either phase delay ( $\tau_p$ ) or relative modulation ( $\tau_m$ ) are equal at all frequencies. When the emission is heterogeneous and given for excitation by a pulse as a sum of exponentials

$$I(t) = \sum_{i=1}^n A_i \exp(-t/\tau_i) \quad (1)$$

in which the  $A_i$  are amplitudes and  $A_i > 0$ , the observed  $\tau_p$  and  $\tau_m$  obtained under sinusoidal excitation differ and are given by

$$\tau_p = \omega^{-1} \tan \langle \phi \rangle \quad (2)$$

$$\tau_m = \omega^{-1} (M_r^2 - 1)^{1/2} \quad (3)$$

where

$$\tan \langle \phi \rangle = \frac{\sum_{i=1}^n \alpha_i \sin \phi_i \cos \phi_i}{\sum_{i=1}^n \alpha_i \cos^2 \phi_i} \quad (4)$$

$$M_r^2 = \left( \sum_{i=1}^n \alpha_i \sin \phi_i \cos \phi_i \right)^2 + \left( \sum_{i=1}^n \alpha_i \cos^2 \phi_i \right)^2 \quad (5)$$

In the above expressions,  $\omega = 2\pi f$  ( $f$  = modulation frequency),  $\phi_i$  is the phase angle of the  $i$ th component with lifetime  $\tau_i$ , and  $\alpha_i = A_i\tau_i/\sum A_i\tau_i$  is the fractional steady-state intensity due to the  $i$ th component ( $\sum \alpha_i = 1$ ). The  $\tau_p$  and  $\tau_m$  data were obtained at two modulation frequencies and analyzed for two exponential components by a procedure in which  $\chi^2$  is defined by

$$\chi^2 = \sum_{\omega} \left[ \left( \frac{\tau_p^t - \tau_p}{\sigma_p} \right)^2 + \left( \frac{\tau_m^t - \tau_m}{\sigma_m} \right)^2 \right]$$

and minimized by varying the  $\alpha_i$  and  $\phi_i$ .  $\tau_p^t$  and  $\tau_m^t$  are the theoretical phase and modulation lifetimes calculated according to eq 2–5, and  $\sigma_p$  and  $\sigma_m$  are the estimated standard deviations of the measured lifetimes. Further details of the heterogeneity analysis are discussed elsewhere (A. M. Kleinfeld and E. D. Matayoshi, unpublished experiments).

For all lifetime measurements, an excitation polarizer set at 35° from the vertical was used in order to eliminate the effects of Brownian rotations (Spencer & Weber, 1970). A monochromator was employed for excitation (342 nm, 1-nm band-pass). The fluorescent samples were always checked against a blank containing all components except the probe, and when necessary, appropriate corrections for scattering contributions were performed. One can show from eq 4 and 5 that at the modulation frequencies used here the lifetime determination of a long-lived fluorophore ( $\tau \approx 100$  ns) is sensitive to small amounts of contaminating scatter in the detected signal. For this reason (and because of the limited number of frequencies available), emission filters were found to be inadequate in the front-surface lifetime measurements. When a monochromator was used in the emission channel, scattering from PBA- or PBC-labeled red cells was reduced to less than 0.1% of the fluorescence signal.

For measurements on intact cells, the large absorbance due to hemoglobin at both excitation and emission wavelengths effectively limits the observed fluorescence to no more than two or three layers of cells at the front surface of the cuvette. (The optical transmission at 384 nm through a single spherical echinocyte of diameter 5.7  $\mu$ m is only 40%.) Although PBA and PBC fluoresce in aqueous buffers, their extremely large membrane partition coefficients alone imply that free probe (i.e., extracellular plus intracellular probe not bound to the membrane) constitutes no more than 1–2% of the total probe present in samples of packed cells. This expectation was tested by adding an aqueous quencher such as  $I^-$  to PBA-labeled intact cells. We have found  $I^-$  to be an efficient collisional quencher of pyrene fluorescence in aqueous dispersions of PBA and PBC (unpublished observations), in agreement with previous studies on PBA (Chen, 1974). Red cells (5% suspension) were incubated for 1 h at 37 °C in a 20 mM Tris-buffered (pH 7.4) solution of 150 mM NaI. The solution was freshly prepared, flushed with nitrogen, and also contained 2 mM  $Na_2S_2O_3$  to minimize  $I_3^-$  formation.  $I^-$  reaches the intracellular aqueous compartment via band 3, the anion-exchange protein of the red cell membrane (Cabantchik et al., 1978). Since a negligible effect on the fluorescence decay was observed, we conclude that the contribution of free probe is in fact less than 1% of the total signal intensity and that quenching of intracellular free probe by hemoglobin may additionally be occurring.

## Results and Discussion

**Effect on Cell Shape.** When intact human erythrocytes are incubated in the presence of low concentrations (4–100  $\mu$ M)

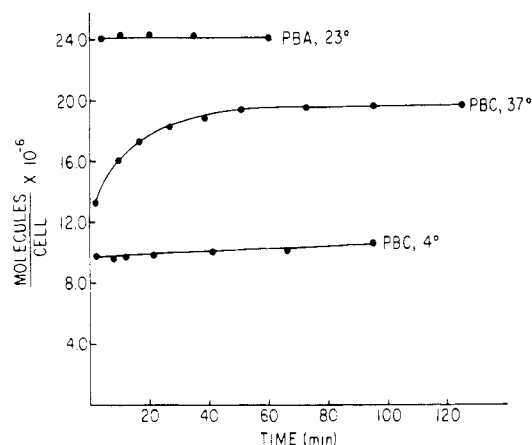


FIGURE 1: Uptake of PBA and PBC by intact red cells. Curve labeled "PBA, 23°": uptake of PBA at 23 °C; 42  $\mu$ M PBA, 7.6% hematocrit. Curve labeled "PBC, 37°": uptake of PBC at 37 °C; 13.6  $\mu$ M PBC, 2.3% hematocrit. Curve labeled "PBC, 4°": uptake of PBC at 4 °C; 14.7  $\mu$ M PBC, 2.7% hematocrit. In each instance, washed red cells were suspended in 10 mM sodium phosphate–150 mM NaCl, pH 7.4, at the indicated temperature, hematocrit, and final concentration of PBA or PBC. See Materials and Methods for further details.

of either PBA or PBC, their normal biconcave disk shape immediately becomes crenated. As observed with other nonspecific amphiphilic compounds, the severity of the echinocytic transformation increases with increasing concentration of compound in the medium, and if distortion is not carried out to the spherocyte stage, the effects can be reversed by washing the treated cells with probe-free buffer. Neither butyric acid nor butyrylcholine, lacking the nonpolar pyrene moiety, has any effect on cell shape at 10 mM concentrations.

Further investigation revealed several interesting differences between the effects of PBA and PBC. First of all, it was observed that PBA-treated cells could not be distorted beyond the spherocochinocyte I stage at the highest concentrations testable (maximum solubility of PBA in aqueous solutions is approximately 100  $\mu$ M). PBC-treated cells were easily transformed beyond this stage and also at 5-fold lower concentrations. This was a curious finding, because subsequent measurement of probe binding to unsealed ghosts indicated that the membrane partition coefficient of PBC is at most only 1.5–2 times larger than PBA (see below), implying that much less PBC per cell was needed to distort the shape to a particular echinocyte morphology.

Another important difference was that the morphology of PBC-treated cells was dependent on the time and temperature of the incubation period; PBA-induced crenation was independent of these conditions. The spherocochinocytes obtained by PBC treatment will slowly revert back toward the discocyte morphology when incubation is carried out at 37 °C for at least 1–2 h. The shapes observed after this period depend on the hematocrit and initial PBC concentration but are quite heterogeneous within any particular sample (mixtures of discocytes, echinocytes II and III, and some stomatocytes). The extent of shape reversal also seems to be somewhat greater with old or outdated bank blood. But irrespective of the blood source, these reversals of the initial spiculation occur much more slowly if incubations are carried out at room temperature and fail to occur at all if incubation is at 4 °C.

The results shown in Figure 1 indicate that the uptake of PBA and PBC by intact cells is correlated with the effects of the incubation conditions. The uptake was measured by the reduction of probe concentration in the supernatant. Incubation with PBC at 37 °C results in a slow increase in uptake from  $13.2 \times 10^6$  PBC/cell after 2 min, to  $19.4 \times 10^6$  PBC/cell

Table I: Lifetimes of PBA and PBC in Ghosts and Intact Red Cells<sup>a</sup>

	measured lifetimes				heterogeneity analysis				
	$\tau_m(6)$	$\tau_p(6)$	$\tau_m(18)$	$\tau_p(18)$	$\alpha_1$	$\tau_1$	$\alpha_2$	$\tau_2$	$\chi^2$
PBA									
ghosts <sup>b</sup>	130 ± 1	129 ± 4	129 ± 3	125 ± 8	1.00	130			
intact cells <sup>c</sup>	99 ± 1	73 ± 5	88 ± 2	36 ± 5	0.97	102 ± 2	0.03	8 ± 2	0.046
PBC									
ghosts	143 ± 1	138 ± 8	<i>d</i>	<i>d</i>	1.00	143			
intact cells	108 ± 2	86 ± 10	91 ± 6	62 ± 8	0.96	114 ± 1	0.04	17 ± 1	2.2

<sup>a</sup> Modulation and phase lifetimes were obtained at two modulation frequencies, 6 and 18 MHz or 10 and 30 MHz. The error shown is the estimated standard deviation obtained from at least 20 measurements, each of which is an average of 10 measurements. The measurements were performed at 23 °C, and samples were not deoxygenated. All lifetimes are in ns. The  $\chi^2$  values are normalized to the number of degrees of freedom, which is 1 for these two-component fits. Fits are deemed satisfactory for values of  $\chi^2$  less than 1.64, which corresponds to a probability of 0.2. <sup>b</sup> Lifetimes of ghosts were determined at 10 and 30 MHz, not 6 and 18 MHz. The emission was isolated with a Corning 4-96 filter. <sup>c</sup> Lifetimes of intact cells were measured at an emission wavelength of 382 nm with a 16-nm monochromator band-pass. <sup>d</sup> Not determined.

after 51 min whereas incubation at 4 °C prevents any further uptake beyond the initial binding. In contrast to PBC uptake, the binding of PBA to intact cells shows complete equilibration within the first few minutes at all temperatures.

Two further observations with PBC are of particular interest. First, if intact cells which have been incubated at 37 °C for 2 h with PBC are now washed rapidly with an excess of cold, PBC-free buffer and then fixed, they are found to be nearly homogeneously cupped. Second, the treatment of unsealed, hemoglobin-free ghosts (in 10 mM Tris and 25 mM NaCl, pH 7.5) with PBC (10–50  $\mu$ M) resulted in strongly cupped ghosts, in contrast to the echinocytes induced in intact cells.<sup>2</sup> These results are similar to the shape-changing effects of the positively charged drug methochlorpromazine found by Sheetz & Singer (1974, 1976).

As suggested by the latter authors for the effects of chlorpromazine and methochlorpromazine, the results with PBA and PBC can be rationalized by assuming that PBA, possessing a titratable carboxylate, can rapidly diffuse across the membrane as the neutral species, but PBC, possessing a permanently charged quaternary amine, is very poorly permeable. The observation that binding to unsealed ghosts is rapid for both pyrene derivatives at all temperatures is consistent with this explanation. Furthermore, while the amount of PBA bound per cell is nearly comparable for ghosts and intact cells, the amount of PBC bound per intact cell is less than half that bound per ghost. The apparent membrane partition coefficient observed depends on the amount of bound probe; when ghosts (between 100 and 500  $\mu$ g of protein/mL) are incubated with 50–25- $\mu$ M probe,  $K_p$  (membrane concentration/aqueous phase concentration) varies between 3000 and 3600 for PBA and between 4900 and 6600 for PBC. As is commonly observed with the binding to membranes of other charged compounds such as 8-anilino-1-naphthalenesulfonate (Fortes & Hoffman, 1971; Fortes, 1976), an apparent decrease in affinity occurs as the amount of bound dye increases, implying that bound dye creates an electrostatic surface potential which repels the binding of subsequent molecules.

<sup>2</sup> Treatment of well-washed ghosts with PBA had virtually no effect on ghost shape. This was not entirely surprising, however, since there appears to be a similar lack (or decreased sensitivity) of ghost shape response to other crenating agents (unpublished observations). Bieri et al. (1974) also noted a lack of effect on the shape of ghosts treated with nitroxide stearates—compounds which crenate intact red cells. It is unclear at present why drug-induced cupping, but not drug-induced crenation, should be readily elicited in ghosts since both echinocytic and stomatocytic ghosts are obtainable by simply manipulating the ionic milieu of the suspending medium (unpublished observations; Vaughan & Penniston, 1976; Johnson & Robinson, 1976).

Table II: Effect of Heterogeneity on  $\tau_m$ - $\tau_p$  Splitting<sup>a</sup>

$\alpha_2$	$\tau_m(6)$	$\tau_p(6)$	$\tau_m(18)$	$\tau_p(18)$
0	102	102	102	102
0.005	101.46	95.59	99.31	76.12
0.01	100.91	89.94	96.68	61.27
0.02	99.73	80.46	91.63	44.90
0.05	95.75	61.18	78.30	26.76
0.10	88.24	43.83	61.73	17.84

<sup>a</sup> Calculated effect on phase and modulation lifetimes (6 and 18 MHz) of variable amounts of a 7.8-ns component in the presence of a 102-ns main component.  $\alpha_2$  = fractional intensity of the  $\tau_2$  = 7.8-ns component. (These values of  $\tau_1$  and  $\tau_2$  were chosen from the analysis of the PBA-intact cell data.)

In the sections which follow, we present evidence from fluorescence measurements which supports the hypothesis (Sheetz & Singer, 1974) that a partitioning of amphiphiles into the outer bilayer half is associated with crenation whereas a partitioning into the inner half is associated with cupping of the normal discocyte shape.

**Lifetime Measurements.** The measurement of fluorescence lifetimes was undertaken in an attempt to quantitate the distribution of bound probe between the two halves of the membrane. We found that the lifetimes of PBA and PBC in hemoglobin-free ghosts were virtually homogeneous (Table I) and therefore anticipated that in *intact* cells the large concentration of hemoglobin might provide an intrinsic means of identifying the fluorescence from probe molecules bound at the cytoplasmic surface. Nonradiative energy transfer from pyrene to hemoglobin should occur because of the large spectral overlap of pyrene emission with heme absorption. The time-resolved fluorescence emission should therefore minimally display a long-lifetime component corresponding to unquenched (or poorly quenched) outer membrane half fluorophores and a shorter component corresponding to highly quenched inner half fluorophores.

The phase and modulation lifetimes for intact red cells labeled with PBA are shown in Table I. The results presented are from one experiment, but very similar results were obtained in three other experiments. The large splittings in the phase and modulation lifetimes indicate the presence of short components. An analysis of the four phase and modulation lifetimes showed that the decay could be fit well as the sum of two exponentials, with fractional intensities and lifetimes as indicated to the right in the table. It should be noted that because of the modulation frequencies employed in this study ( $f = 6$  or 18 MHz), there is a particularly enhanced sensitivity to small fractions of short-lifetime components ( $\tau \approx 1/(2\pi f)$ ) in the presence of a primary long-lifetime component ( $\tau \gg$

$1/(2\pi f)$ ). Thus, the determined  $\alpha_2 = 3\%$  is highly significant because of the particular combination of lifetimes and modulation frequencies. To clarify this point, we have presented in Table II the (calculated) values of  $\tau_p$  and  $\tau_m$  which would be observed for values of  $\alpha_2$  ranging from 0 to 10%.

Lifetime measurements of PBC bound to red cells are also displayed in Table I. In contrast to the results with PBA, analysis of the PBC data as the sum of two exponentials yielded poor  $\chi^2$  fits in each of four experiments. The decay complexity is perhaps not surprising in the case of PBC because the decay of the monomer fluorescence in a viscous medium such as a membrane can be nonexponential when excimer formation is also occurring (Vanderkooi & Callis, 1974). Whether this effect underlies the observed decay in the present case could not be determined since (1) PBC excimers form readily at low concentrations and poor sample intensities prevented acquisition of sufficiently accurate lifetime data at concentrations where excimer formation is negligible and (2) measurements could be performed at only two modulation frequencies. By contrast, as will be noted below, excimer formation was very inefficient in PBA-labeled cells. Lifetime measurements of either PBA or PBC bound to ghosts could be done at probe concentrations 10–100-fold lower than those used for intact cells, and excimer fluorescence was entirely absent.

It should be emphasized that in these lifetime measurements the background intensity (of a sample of unlabeled erythrocytes) was less than 0.1%, which excludes the possibility of artifactual lifetime components arising from scatter or from fluorescent contaminants in the erythrocytes themselves. We were also well aware of an artifactual component ( $\tau \approx 10$  ns) which can sometimes be produced in PBA samples during the measurements by high excitation intensities or by exposure of samples to excessive temperatures (Spencer et al., 1969). However, such artifacts can be ruled out because under our conditions homogeneous lifetimes could be obtained in either aqueous dispersions of PBA or hemoglobin-free ghosts labeled with PBA.

Finally, we can eliminate the possibility that the short component arises from (1) extracellular or intracellular free dye or (2) intracellular dye adsorbed to hemoglobin. Simple calculation, based on the measured partition coefficient, the packed cell hematocrit, and, for the second case, the difference between the partitioning into hemoglobin-free ghosts and intact cells, shows that if  $\tau_2$  corresponded to any of these components  $\alpha_2$  must have a value less than 0.2%. This estimate does not take into account fluorescence quenching by nonradiative transfer to hemoglobin, which will reduce even further the possible contribution by either type of intracellular component.

In view of these considerations, we conclude that the highly quenched 8-ns component in intact cells must arise from those PBA molecules located in the inner bilayer half. PBA to heme energy transfer is expected to be efficient since the calculated Förster parameter  $R_0$  (the donor to acceptor distance at which energy transfer takes place with 50% efficiency) is 43.5 Å, based on an orientation factor of  $\kappa^2 = 2/3$  (Matayoshi, 1979). With an  $R_0$  of this magnitude, some quenching of the outer bilayer half fluorophores might also be expected; indeed,  $\tau_1$  for PBA in intact cells was found to be smaller than the single lifetimes of 130 ns obtained in hemoglobin-free ghosts (Table I). If we assume that  $\tau = 130$  ns represents the unquenched lifetime of membrane-bound PBA and use the values of  $\tau_1 = 102$  ns and  $\tau_2 = 8$  ns to estimate a lower limit for the transfer efficiency, apparent distances of 54 and 27 Å are obtained.<sup>3</sup>

Table III: Paramagnetic Quenching of PBA Bound to Intact Red Cells<sup>a</sup>

addition	$\alpha_1$	$\tau_1$	$\alpha_2$	$\tau_2$	$\chi^2$
5 mM Ca <sup>2+</sup>	0.97	102	0.03	7.8	0.046
5 mM Mn <sup>2+</sup>	0.93	75	0.07	8.3	0.40
5 mM Mn <sup>2+</sup> , 10 mM EDTA <sup>b</sup>	0.96	97	0.04	8.6	0.55

<sup>a</sup> Two-component heterogeneity analysis of modulation and phase lifetimes measured at 6 and 18 MHz and performed as described in the text and under Table I. All lifetimes are in ns.

<sup>b</sup> EDTA = ethylenediaminetetraacetic acid.

If these values approximate minimum transfer distances along a vector normal to the plane of the bilayer (achieved by diffusion during the lifetime of PBA), the relative difference of 27 Å is reasonably consistent with the expected transbilayer vertical distance separating PBA molecules located at the two membrane surfaces.

Since the  $\alpha$ 's in Table I are intensity-weighted fractions, the molar ratio of inside to outside PBA molecules is not  $\alpha_2/\alpha_1$  but  $(\alpha_2/q_2)/(\alpha_1/q_1)$ . This leads to the conclusion that  $29 \pm 4\%$  of the membrane-bound PBA is in the inner bilayer half with a lifetime of 8 ns and  $71 \pm 4\%$  is located in the outer half with a lifetime of 102 ns, assuming that  $q_1/q_2 = \tau_1/\tau_2$ .

These findings directly support the idea that echinocytes result from an asymmetrical expansion of the outer bilayer half relative to the inner half. The 71:29 distribution is also of interest because, as noted earlier, much more PBA/cell than PBC/cell is required to produce the equivalent echinocyte morphology: approximately  $38 \times 10^6$  PBA/cell and  $22 \times 10^6$  PBC/cell each produced cells bearing the spheroechinocyte I morphology, and  $10 \times 10^6$  PBA/cell and  $6 \times 10^6$  PBC/cell each produced echinocyte II's. If the distribution of PBC across the bilayer during the first few minutes of incubation is essentially 100:0 (outer/inner) (due to its low permeability) while the distribution for PBA is 71:29, the greater efficacy of PBC is not surprising.<sup>4</sup> Hence, these results emphasize that it is both the concentration of compound in the membrane and the asymmetry of its distribution between the bilayer halves which determine red cell shape.

**Paramagnetic Quenching of PBA.** We attempted to obtain further evidence concerning the identity of the two components by examining the effect of the paramagnetic cation Mn<sup>2+</sup> on the fluorescence heterogeneity. Mn<sup>2+</sup> has been used in nuclear magnetic resonance studies of phospholipid vesicles as a nonpenetrating agent which binds at the lipid phosphate groups (Bergelson, 1978). Since paramagnetic quenching of fluorescence requires a minimum interaction distance of about 4–6 Å (Green et al., 1973), it was anticipated that Mn<sup>2+</sup> might quench membrane-bound PBA.<sup>5</sup> Intact human erythrocytes

<sup>3</sup> Apart from the question as to the validity of assuming dynamic averaging conditions, it should perhaps be mentioned that in general it is insufficient to use merely the ratio of quenched and unquenched lifetimes in order to calculate the PBA to heme distance. The apparent distance obtained may be an overestimate because one must consider the effect of donor and acceptor diffusion (Elkana et al., 1968) during the long lifetime of PBA as well as the presence of more than one acceptor per donor (e.g., Shaklai et al., 1977). We have not attempted here to use or discuss either calculation since given the large uncertainties in our case no further light would be cast on the interpretation.

<sup>4</sup> Quantitative verification that the ratio  $A_o/A_i$  (where  $A_o$  = surface area of the outer bilayer half and  $A_i$  = surface area of the inner half) is the same for the cited cases is not easily obtained because  $A_o/A_i$  is sensitive to the value assumed for the volume per probe molecule and the exact distribution assumed. Use of the van der Waals molecular volume is unacceptable in view of the data of Seeman and co-workers, which implies that the expanded membrane volume may be as much as 10-fold greater than the bulk volume occupied by the drug (Seeman, 1972).

from freshly drawn blood are impermeable to low concentrations ( $\leq 10$  mM) of  $\text{Mn}^{2+}$ , within the several minutes required to perform the lifetime measurements (J. A. Dix and A. K. Solomon, unpublished results). Thus, if the preceding explanation for the observed PBA heterogeneity is correct,  $\text{Mn}^{2+}$  should only quench the long (102-ns) lifetime component.

The results of such an experiment are shown in Table III. Measurement of the phase and modulation lifetime splittings at 6 and 18 MHz, as performed in the preceding section, demonstrated that the addition of 5 mM  $\text{MnCl}_2$  to PBA-labeled cells caused quenching of  $\tau_1$  from 102 to 75 ns. This quantitative quenching of  $\tau_1$  supports the inference, from energy-transfer considerations, that there can be no probe molecules with  $\tau \gg 7.8$  ns at the inner bilayer half because of its proximity to intracellular hemoglobin. By comparison, it is interesting to note that the addition of 5 mM  $\text{Mn}^{2+}$  to an aqueous solution of PBA (in the absence of red cells, not deoxygenated) caused a reduction in  $\tau$  from 96 to 59 ns.

The interpretation of the results with respect to compound 2 is unfortunately less certain. While  $\tau_2$  appears to remain constant after addition of  $\text{Mn}^{2+}$  (Table III), the conclusion that it is necessarily more shielded from  $\text{Mn}^{2+}$  than component 1 is ambiguous because of the shortness of  $\tau_2$ , the low efficiency of the  $\text{Mn}^{2+}$  quenching reaction, and the precision of  $\tau_2$ . If both components are equally accessible to the quencher and obey Stern-Volmer kinetics, then

$$q_0/q = 1 + k\tau_0[Q]$$

where  $q_0$  and  $q$  are quantum efficiencies of the fluorophore in the absence and presence of quencher,  $[Q]$  is the concentration of quencher,  $\tau_0$  is the lifetime of the fluorophore in the absence of quencher, and  $k$  is the bimolecular (diffusion-controlled) collisional rate constant. If it is further assumed that  $q_0/q = \tau_0/\tau$ , the quenching observed for the long component (102 ns/75 ns) implies that under identical conditions  $\tau_2$  should be quenched from 7.8 to 7.6 ns. Since the propagated error on  $\tau_2$  from the heterogeneity analysis is much larger (Table I), it is clear that we will not be able to detect conclusively the quenching of  $\tau_2$  for such low values of the product  $k[Q]$ .

Two different controls are also indicated in Table III. First, the replacement of  $\text{Mn}^{2+}$  with nonparamagnetic  $\text{Ca}^{2+}$  (also impermeant to red cells) was found to have no effect on the phase and modulation lifetimes. This implies that the quenching of membrane-bound PBA by  $\text{Mn}^{2+}$  is not simply an indirect effect of the structural perturbation of the membrane by the divalent cation. Second, the addition of an excess of EDTA is shown to reverse almost completely the effect of  $\text{Mn}^{2+}$ . This result confirms the assumption that membrane-bound  $\text{Mn}^{2+}$  is indeed quenching membrane-bound PBA since EDTA- $\text{Mn}^{2+}$  complexes are as effective as  $\text{Mn}^{2+}$  alone in quenching free, aqueous PBA (not shown).

It is to be noted in Table III that the values of the fractional intensities obtained after  $\text{Mn}^{2+}$  addition do not change in proportion to the reduced  $\tau$ 's, i.e.,  $(q_1/q_1)^{\text{Mn}} \neq (\tau_1/\tau_1)^{\text{Mn}}$ . It has been suggested that the mechanism of paramagnetic quenching involves either enhanced singlet-triplet crossover

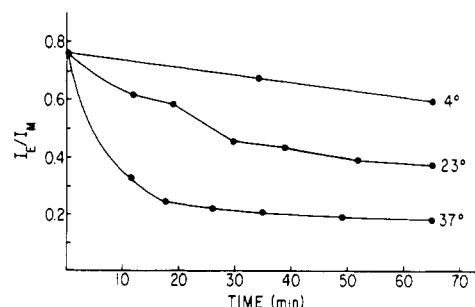


FIGURE 2: Loss of PBC excimer fluorescence. Washed erythrocytes were suspended at 4 °C in 10 mM Tris-150 mM NaCl, pH 7.4, containing 60  $\mu\text{M}$  PBC and at a final hematocrit of about 7%. The suspension was pelleted within seconds, and the packed cells (separated from the supernatant) were incubated at either 4, 23, or 37 °C. At the various times indicated, the cells were removed, and  $I_E/I_M$  was measured at 23 °C.  $I_E$  = the excimer intensity, observed at 490 nm;  $I_M$  = the monomer intensity, measured at 396 nm. Excitation was at 348 nm, and the monochromator band-passes were 2 nm (excitation) and 8 nm (emission). See Materials and Methods for further details.

or vibrational coupling of the donor and acceptor (Green et al., 1973). If the latter takes place, it is indeed possible that the radiative rate constant has been altered in the presence of  $\text{Mn}^{2+}$ , thus bringing about disproportionate changes in quantum yield vs. lifetime. Alternatively, the apparent  $\alpha$ 's might reflect a truly altered partitioning of PBA between the two bilayer halves as a result of the increased positive charge present at the extracellular surface. However, this possibility does not alter the conclusion that the long-lifetime component corresponds entirely to PBA molecules located in the outer bilayer half.

**Excimer Fluorescence of PBC.** The excimer fluorescence displayed by pyrene and its derivatives has conveniently been used in several studies to obtain information concerning the viscous properties of membranes. The excimer ratio (ratio of the excimer to monomer quantum efficiencies) is proportional to both the pyrene concentration and its diffusion rate (Birks et al., 1963; Galla & Sackman, 1974). In the present work, advantage was taken of this property in order to seek further evidence on the question of whether the slow equilibration of PBC with intact cells involves a redistribution of bound molecules between the bilayer halves.

The efficiency of excimer formation by charged pyrene derivatives in membranes is considerably lower than underivatized pyrene (Vanderkooi & Callis, 1974). Furthermore, the high cholesterol content of red cell membranes is expected to reduce the capacity for excimer formation. Nonetheless, at the concentrations needed to perturb the red cell shape, substantial excimer formation was observable with PBC at 23 °C. In contrast, PBA-labeled cells displayed very low excimer fluorescence at the highest concentrations. The difference in the efficiency of excimer formation between PBA and PBC is evidently due to differences in their lateral diffusion rates in red cell membranes since a similar difference was not observable when the two probes were dissolved in a simple isotropic solvent such as *N,N*-dimethylformamide (data not shown).

Figure 2 shows the observed excimer ratio as a function of time when packed red cells, labeled with PBC, are incubated at 4, 23, and 37 °C. At each data point, the cuvette containing the packed cells was inserted into the front surface holder (at 23 °C), and the emission intensities at 396 (monomer) and 490 nm (excimer) were obtained. As seen in Figure 2, the excimer formation is initially large, but is rapidly reduced if cells are incubated at 37 °C, occurs much less rapidly at 23 °C, and is reduced very little at 4 °C. In contrast, the low

<sup>5</sup> In the present application, it is not known whether the quenching efficiency is greater than the essentially collisional quenching observed in free solution—if in fact we are dealing with a longer range interaction between planar arrays of paramagnetic quenchers and fluorophores—or whether quenching occurs because of actual permeation of divalent paramagnetic ions into the hydrophobic regions of the bilayer, as recently suggested by Thulborn & Sawyer (1978).

excimer ratio ( $<0.2$ ) observed from PBA-labeled cells shows none of these time- or temperature-dependent changes.

When interpreting these results, one should bear in mind the following. The packed cells have been separated from the initial labeling solution so that further uptake of dye after  $t = 0$  is minimal. Furthermore, the excimer emission can *only* arise from membrane-bound dye. Aqueous concentrations in excess of  $10^{-3}$  M would be required in order to exhibit excimer fluorescence; the high partition coefficient of PBC results in a calculated overall membrane concentration greater than 35 mM in the experiment of Figure 2. Finally, one would expect a low efficiency for excimer formation from dye bound at the inner bilayer half because of efficient quenching of the monomer excited-state lifetime via energy transfer to hemoglobin. The lifetime measurements on PBA discussed above indicate that the fluorescence lifetime of pyrene molecules bound at the inner bilayer half is quenched more than 10-fold. Therefore, the observed excimer emission should be overwhelmingly due to PBC bound in the outer bilayer half.

From these considerations, we conclude that the observed reduction of excimer emission in time must involve a diluting of PBC molecules initially concentrated in the outer bilayer half. Permeation of probe molecules across the bilayer would produce a net depletion of the outer bilayer half population. The resulting increase of probe concentration in the inner bilayer half would not give rise to a compensating excimer intensity, for reasons just noted.

Consistent with this explanation is the observation that, if the incubation at 37 °C is performed at *low hematocrit* (i.e., with the original labeling solution) and a sample of cells is pelleted at intervals for fluorescence measurements, then a decrease of the initial excimer ratio is not observed. Under such conditions, a reduction of probe concentration in the outer bilayer half cannot occur because it is always in equilibrium with a large excess of free PBC.

An alternative explanation for the apparent fourfold reduction in probe concentration at 37 °C (inferred from Figure 2) is that all PBC molecules are bound initially in the outer bilayer half in clusters but subsequently become randomly distributed within the outer half without permeating the bilayer. Such a possibility seems highly unlikely, especially in view of the difference in the uptake of PBC between unsealed ghosts and intact cells and the rapid equilibration of PBC with the ghosts under all conditions.

The excimer results thus provide an explanation for the time-dependent morphological changes which occur when the cells are incubated for extended periods with PBC. When the cells are incubated with PBC at 4 °C, the PBC remains concentrated in the outer bilayer half. However, at 37 °C, a significant number of PBC molecules can permeate and equilibrate with the inner surface. The initially observed echinocytic shape is therefore associated with intercalation of PBC in the outside bilayer half, and the (stomatocytic) reversal is associated with the increased partitioning into the inner half. Similarly, when the 37 °C, 2-h-incubated cells are rapidly washed in cold buffer, PBC bound in the outer bilayer half is largely depleted before PBC molecules in the inner half have had time to reequilibrate. The inner half is thereby left relatively expanded, and the stomatocytic reversal is accentuated (compared to the reversal witnessed in the absence of the cold washout). This explanation was originally suggested by Sheetz & Singer (1976) and is strongly supported by our results.

**Hemolysis Protection.** Quantitation of the degree to which anesthetics, drugs, and other organic compounds protect red blood cells against hypotonic hemolysis has frequently been

used to study the interaction of these compounds with membranes. It was therefore of further interest to see whether changes in cell shape induced by PBC or PBA were correlated with osmotic fragility. Both crenating and cup-forming amphiphiles can protect red cells against hemolysis up to a certain optimal concentration, and above this concentration cells become spherical and hemolytically more fragile (Seeman, 1972; Lovrien et al., 1975). Protection against hypotonic hemolysis by these compounds appears to be a consequence of the increased cell surface area/volume ratio. Both PBA and PBC are presumably anchored at the membrane-water interfaces, and the symmetry or asymmetry of their distribution between the two bilayer halves would be expected to affect the extent and stability of the expanded bilayer. Changes in relative hemolytic protection during incubations with probe might therefore be indicative of changes in the total amount bound and/or a redistribution of probe between the inner and outer halves of the membrane.

Figure 3A,B shows the concentration dependence of hemolysis for PBA and PBC after incubation with the indicated concentration of probe at room temperature for 10 min. Figure 3C shows the change in relative hemolysis as a function of time of incubation at 37 °C at concentrations of 20 and 40  $\mu$ M PBC. In addition, the cell shape was examined by light microscopy and is indicated at various concentrations or time points in the figures. In each case, the correlations between cell morphology and the shape of the hemolysis curves were reproduced in at least three experiments.

Several features are noteworthy. It was observed, in agreement with previous workers (Bieri et al., 1974; Lovrien et al., 1975; Fortes & Ellory, 1975), that maximal membrane stabilization is afforded by conditions which produce spiculation of red cell shape. For example, in the biphasic hemolysis curve of PBC, typical of those frequently obtained with other amphiphilic compounds (Seeman, 1972), the cells are largely echinocyte III to spherocyte I at the minimum in the curve. At higher PBC concentrations, the cells become increasingly fragile and acquire the smooth spherical appearance of the spherocyte II. In Figure 3A, and PBA hemolysis curve may be approaching a minimum (based on the low relative hemolysis value) at the largest (solubility limiting) concentrations, and again, the cell morphology is that of the echinocyte III to spherocyte I.

In Figure 3C, red cells which are initially spherocyte II are seen to become dramatically stabilized against hemolysis. As is apparent from the hemolysis-concentration curve of Figure 3B, an increase in bound probe alone should only make the cells *more* fragile. These results therefore imply that a large redistribution of PBC within the bilayer must accompany the slow uptake of probe, in agreement with the interpretation of the excimer and uptake measurements.

As in the uptake measurements, cells incubated at 4 °C with PBC show no change in either relative hemolysis or morphology, and cells tested with PBA at 37 °C show no changes with time.

## Conclusions

The results of the experiments described here indicate that the effects of the two pyrene derivatives PBA and PBC on red cell shape depend on their relative concentrations in the two halves of the bilayer. The fluorescence lifetime measurements provide a quantitative assessment of the asymmetrical membrane distribution of PBA while the excimer measurements of PBC directly demonstrate that a decrease in outside/inside ratio of bound probe is correlated with the time-dependent shape changes. The observed effects of PBA and PBC on the

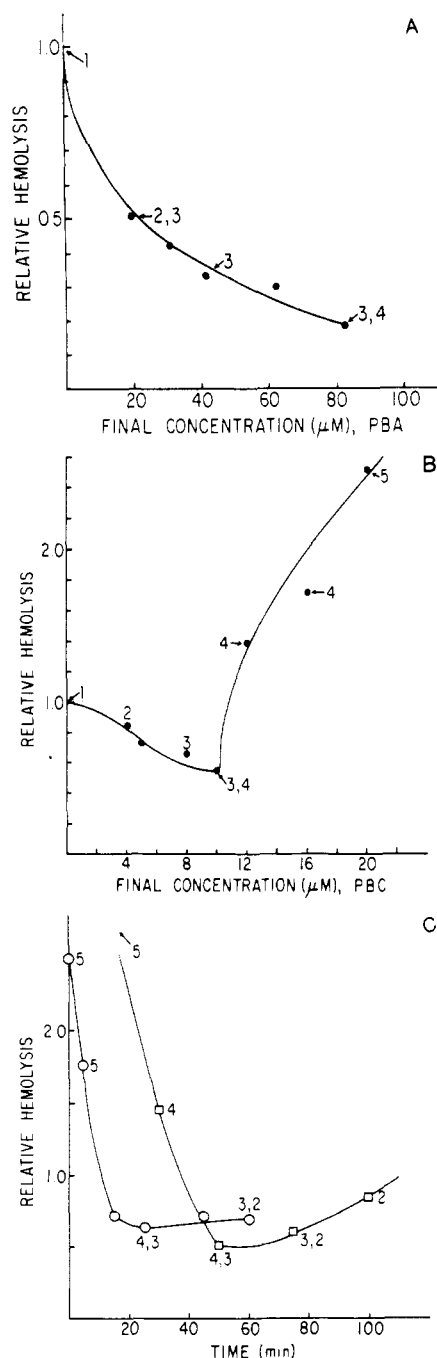


FIGURE 3: Hemolysis protection by (A) PBA and (B) PBC. Red cells were incubated with various concentrations of PBA or PBC for 10 min at 23 °C and then tested for hemolysis protection as described under Materials and Methods. A nonhemolyzed sample of cells at each concentration was removed, fixed with glutaraldehyde, and examined by light microscopy. The numbers at points along the curves indicate the cell shapes observed: 1 = discocyte; 2 = echinocyte II; 3 = echinocyte III; 4 = spherocyte III; 5 = spherocyte IV. (C) Time dependence of hemolysis protection by PBC. Red cells were incubated at 37 °C with 20 (○) or 40 μM PBC (□). At the times indicated, a sample of cells was removed, briefly equilibrated (20–30 s) at 23 °C, and tested for hemolysis protection. A nonhemolyzed sample at each time point was fixed with glutaraldehyde and examined by light microscopy.

cellular hemolytic fragility qualitatively support the idea that cell shape and bilayer expansion are intimately related.

Conrad & Singer (1979) have recently reported that when the binding of several amphiphiles (including chlorpromazine) to biological membranes is quantitated by using a new filter method membrane partition coefficients ( $K_p$ ) less than 1 are

obtained. The authors conclude that the apparent values of  $K_p \gg 1$ , obtained by the conventional centrifugation method, reflect a surface absorption (perhaps as micelles) of the amphiphiles. However, it is very unlikely that PBA or PBC is bound in such a manner. The inaccessibility of the membrane-bound fluorophore to lipid-insoluble collisional quenchers such as  $I^-$  and  $Mn^{2+}$ -EDTA complexes (in contrast to the efficient quenching obtained in aqueous dispersions of PBA and PBC) indicates that the hydrophobic pyrene moiety is intercalated into the nonpolar regions of the membrane. In addition, it should be noted that the observed emissive properties of many other commonly used fluorescent membrane probes would be similarly difficult to reconcile with surface absorption of the compound.

The time-dependent shape changes obtained after treatment of red cells with PBC are similar to those which were observed by Sheetz & Singer (1976) for the positively charged drug methochlorpromazine. Measurement of PBA and PBC uptake by intact cells vs. unsealed ghosts demonstrated that the effects of PBC were likely to result from its low membrane permeability. This effect is apparently also the case for methochlorpromazine since Elferink (1977) has shown that chlorpromazine binds equally to unsealed or resealed ghosts but methochlorpromazine binds to unsealed ghosts to a much greater extent. In his studies, the importance of electrostatic factors was demonstrated by the significantly increased binding of either drug to phosphatidylcholine liposomes containing 20% phosphatidylserine, as compared to liposomes without phosphatidylserine.

More recently, Tenforde et al. (1978) attempted to quantitate the asymmetry of chlorpromazine binding to red cells. Their approach was to measure the effect of added chlorpromazine on the cellular electrophoretic mobility. If all chlorpromazine bound in the outer bilayer half is charged, this technique allows direct estimation of the number of chlorpromazine molecules located at the outer surface. Using the value determined by Kwant & Seeman (1969) for the maximal number of available chlorpromazine sites, Tenforde et al. concluded that the outside/inside chlorpromazine distribution ratio is 1:39, thus indicating that the distribution of chlorpromazine is indeed highly asymmetric.

Our findings with PBA and PBC provide further support for the proposal of Sheetz & Singer (1974) that shape changes induced in red cells by amphiphilic molecules are the consequence of an asymmetrical perturbation of the two halves of the bilayer.

#### Acknowledgments

I thank Drs. A. M. Kleinfeld and A. K. Solomon for advice and discussions during the course of this work.

#### References

- Aloni, B., Eitan, A., & Livne, A. (1977) *Biochim. Biophys. Acta* 465, 46.
- Bergelson, L. D. (1978) *Methods Membr. Biol.* 9, 275.
- Bessis, M. (1973) in *Red Cell Shape* (Bessis, M., Weed, R. I., & Leblond, P. F., Eds.) p 1, Springer-Verlag, New York.
- Bessis, M., Weed, R. I., & Leblond, P. F. (1973) *Red Cell Shape*, Springer-Verlag, New York.
- Bieri, V. G., Wallach, D. F. H., & Lin, P. S. (1974) *Proc. Natl. Acad. Sci. U.S.A.* 71, 4797.
- Birks, J. B. (1970) *Photophysics of Aromatic Molecules*, Wiley-Interscience, New York.
- Birks, J. B., Dyson, D. J., & Munro, I. H. (1963) *Proc. R. Soc. London, Ser. A* 275, 575.
- Brecher, G., & Bessis, M. (1972) *Blood* 40, 333.

- Cabantchik, Z. I., Knauf, P. A., & Rothstein, A. (1978) *Biochim. Biophys. Acta* 515, 239.
- Chen, R. F. (1974) *Anal. Biochem.* 57, 593.
- Conrad, M. J., & Singer, S. J. (1979) *Proc. Natl. Acad. Sci. U.S.A.* 76, 5202.
- Deuticke, B. (1968) *Biochim. Biophys. Acta* 163, 494.
- Diem, K., & Lentner, C. (1970) *Scientific Tables*, CIBA-Geigy Ltd., Basel.
- Dodge, J. M., Mitchell, C., & Hanahan, D. J. (1964) *Arch. Biochem. Biophys.* 100, 119.
- Elferink, J. G. R. (1977) *Biochem. Pharmacol.* 26, 2411.
- Elkana, Y., Feitelson, J., & Katchalski, E. (1968) *J. Chem. Phys.* 48, 2399.
- Fortes, P. A. G. (1976) in *Mitochondria, Bioenergetics, Biogenesis, and Membrane Structure* (Packer, L., & Gomez-Puyou, A., Eds.) p 327, Academic Press, New York.
- Fortes, P. A. G., & Hoffman, J. F. (1971) *J. Membr. Biol.* 5, 154.
- Fortes, P. A. G., & Ellory, J. C. (1975) *Biochim. Biophys. Acta* 413, 65.
- Galla, H. J., & Sackmann, E. (1974) *Biochim. Biophys. Acta* 339, 103.
- Gomori, G. (1942) *J. Lab. Clin. Med.* 27, 955.
- Green, J. A., Singer, L. A., & Parks, F. H. (1973) *J. Chem. Phys.* 58, 2690.
- Guidotti, G. (1972) *Arch. Intern. Med.* 129, 194.
- Johnson, R. M., & Robinson, J. (1976) *Biochem. Biophys. Res. Commun.* 70, 925.
- Kwant, W. O., & Seeman, P. (1969) *Biochim. Biophys. Acta* 183, 530.
- Lovrien, R., Tisel, W., & Pesheck, P. (1975) *J. Biol. Chem.* 250, 3136.
- Lowry, O. H., Rosebrough, N. J., Farr, A. L., & Randall, R. J. (1951) *J. Biol. Chem.* 193, 265.
- Matayoshi, E. D. (1979) Ph.D. Thesis, Harvard University, Cambridge, MA.
- Seeman, P. (1972) *Pharmacol. Rev.* 24, 583.
- Shaklai, N., Yguerabide, J., & Ranney, H. M. (1977) *Biochemistry* 16, 5585.
- Sheetz, M. P., & Singer, S. J. (1974) *Proc. Natl. Acad. Sci. U.S.A.* 71, 4457.
- Sheetz, M. P., & Singer, S. J. (1976) *J. Cell Biol.* 70, 247.
- Sheetz, M. P., Painter, R. G., & Singer, S. J. (1976) *J. Cell Biol.* 70, 193.
- Spencer, R. D. (1970) Ph.D. Thesis, University of Illinois, Urbana, IL.
- Spencer, R. D., & Weber, G. (1970) *J. Chem. Phys.* 52, 1654.
- Spencer, R. D., Vaughan, W. M., & Weber, G. (1969) in *Molecular Luminescence* (Lim, E. C., Ed.) p 607, W. A. Benjamin, New York.
- Tenforde, T. S., Yee, J. P., & Mel, H. C. (1978) *Biochim. Biophys. Acta* 511, 152.
- Thulborn, K. R., & Sawyer, W. H. (1978) *Biochim. Biophys. Acta* 511, 125.
- Van Deenen, L. L. M., & DeGier, J. (1974) in *The Red Blood Cell* (Surgenor, D. M., Ed.) Vol. 1, Chapter 4, Academic Press, New York.
- Vanderkooi, J. M., & Callis, J. B. (1974) *Biochemistry* 13, 4000.
- Vaughan, L., & Penniston, J. T. (1976) *Biochem. Biophys. Res. Commun.* 73, 200.
- Zwaal, R. F. A., Roelofsen, B., Comfurius, P., & Van Deenen, L. L. M. (1975) *Biochim. Biophys. Acta* 406, 83.

## Deuterium Magnetic Resonance of Selectively Deuterated Cholesteryl Esters in Phosphatidylcholine Vesicles<sup>†</sup>

Heiner Gorrissen, Alexander P. Tulloch, and Robert J. Cushley\*

**ABSTRACT:** Deuterium nuclear magnetic resonance (<sup>2</sup>H NMR) experiments have been performed on selectively deuterated cholesteryl palmitate (CP) and cholesteryl stearate (CS) in egg phosphatidylcholine (PC) unilamellar vesicles. Egg PC vesicles were found to incorporate up to 5 mol % ester and to have a mean diameter of 22 nm. Addition of 20 mol % cholesterol decreased the solubility of cholesteryl ester in the bilayer to ~2–3 mol %, but the vesicle size remained unchanged. The <sup>2</sup>H NMR results reveal that the acyl chains

of CP and CS are highly disordered ( $S_{CD} < 0.10$ ) both in the presence and in the absence of cholesterol.  $T_1$  measurements for selectively deuterated CP and CS in egg PC vesicles indicate that the high degree of disorder of the ester molecule is not associated with an increase in the rate of gauche-trans chain isomerization. Possible explanations for the low order parameters in terms of molecular motions and orientations are offered.

**T**he onset of atherosclerosis is characterized by rapid accumulation of cholesteryl esters in aortic intimal and medial layers (Cornwell et al., 1975). It has also been reported that the permeability to lactate, iodide, and glucose is much higher

in sclerotic human tissue than in normal tissue (Kirk, 1962). Since a recent study (Forrest & Cushley, 1977) has shown that incorporation of the saturated ester cholesteryl palmitate (CP)<sup>1</sup> increases the permeability of model membranes, data on the structural organization of saturated cholesteryl esters

<sup>†</sup> From the Department of Chemistry, Simon Fraser University, Burnaby, British Columbia V5A 1S6, Canada (H.G. and R.J.C.), and the Prairie Regional Laboratory, National Research Council of Canada, Saskatoon, Saskatchewan S7N 0W9, Canada (A.P.T.). Received November 20, 1979.

<sup>1</sup> Abbreviations used: CP, cholesteryl palmitate; ESR, electron spin resonance; PC, phosphatidylcholine; <sup>2</sup>H NMR, deuterium nuclear magnetic resonance; CS, cholesteryl stearate; rf, radio frequency; DPPC, dipalmitoylphosphatidylcholine.